A CMOS COUPLED NONLINEAR OSCILLATOR ARRAY

Joseph D. Neff[†], *Brian K. Meadows*[†]
Edgar A. Brown[*], *Steve P. DeWeerth*[*], *Paul Hasler*[*]

[†]SPAWAR System Center-San Diego
Code D363

[*]Georgia Institute of Technology
School of Electrical and Computer Engineering

ABSTRACT

This paper details an experimental nonlinear beam-forming array fabricated in a CMOS process. The unit cell oscillator is a nonlinear second order circuit, which demonstrates self-sustaining oscillation. In this paper experimental results from a test oscillator and a linearly coupled array of oscillators are reported. The circuit equations of motion are shown to be equivalent to the van der Pol oscillator, from which a weakly nonlinear phase-amplitude model is derived. This model forms a basis of understanding for the experimental nonlinear beam-forming array.

1. INTRODUCTION

This research is motivated by recent interest in coupled nonlinear oscillator systems and nonlinear beam forming arrays [1][2]. Nonlinear oscillators are constructed and coupled using adjustable wide range amplifiers. By purposefully employing the weak nonlinear properties of the oscillator, a phase-amplitude model is constructed, where the phase and amplitude dynamics are effectively separable. In this mode the CMOS array is a prime candidate for studying coupled nonlinear oscillator arrays. To this end an analytical model of the array is described and experimental results from a beam-forming array are presented.

2. NONLINEAR SECCOND-ORDER SECTION

The oscillator is based on a second order circuit (second order section [3]), shown schematically in figure 1. Several varieties of self-sustaining oscillation can be achieved with this circuit. This study focuses on weak nonlinear oscillation and arrays of coupled weak nonlinear oscillators. Oscillation is achieved by purposefully employing the nonlinear properties of the feedback amplifier (labeled q in figure 1) via an adjustable transconductance range. The amplifier is similar to a wide linear range amplifier (WLA) but allows the width of the linear transconductance region to be adjusted, as well as the overall bias current.

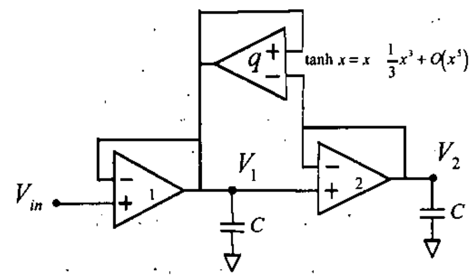

Figure 1. Block diagram of the nonlinear oscillator. The oscillator is a second order system and is constructed from linear and nonlinear amplifiers. The circuit demonstrates weak nonlinear oscillation by employing the inherent nonlinear qualities of the feedback amplifier q. The amplifiers $_1$ and $_2$ operate linearly.

The amplifier design is based on an above-threshold differential pair, whose currents are re-normalized by diodes and a below-threshold differential pair [4]. Equation (1) is used to describe the input-output characteristics of the adjustable WLA. The amplifier linear range and bias current are accessible parameters set by V_l and. V_b respectively. The parameters , , V_t, and I_0 are process dependent parameters, with the values: $=1.32$, $=20.34$, $V_t = 0.62$, $I_0 = 1.47 \quad 10^{15}$ and $C = 4.2 \quad 10^{12}$.

$$I_{out} = B\tanh\left(A(V_+ \quad V\,)\right) \tag{1.0}$$

$$A = \frac{}{V_l \quad V_{l0}} \tag{1.1}$$

$$B = I_0 e^{\ V_b} \tag{1.2}$$

The equations of motion for the circuit can be derived by considering the transconductance of each amplifier, using equations (1.0)-(1.2), and Kirchoff's current law.

$$C\dot{V}_1 = I_1(V_{in}, V_1) + I_q(V_1, V_2) \tag{2.0}$$

$$C\dot{V}_2 = I_2(V_1, V_2) \tag{2.1}$$

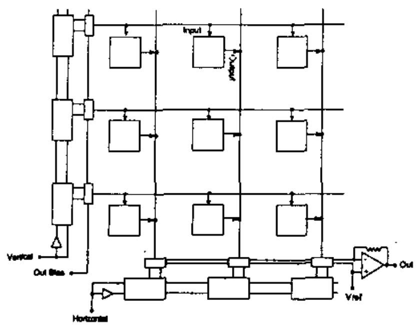

Figure 2. Scanning circuitry block diagram. In the style of Mead et al a row column selection scheme that incorporates horizontal and vertical shift registers and differential current mode output is used [3]. An external operational amplifier is used to convert the scanned current into a measurable voltage.

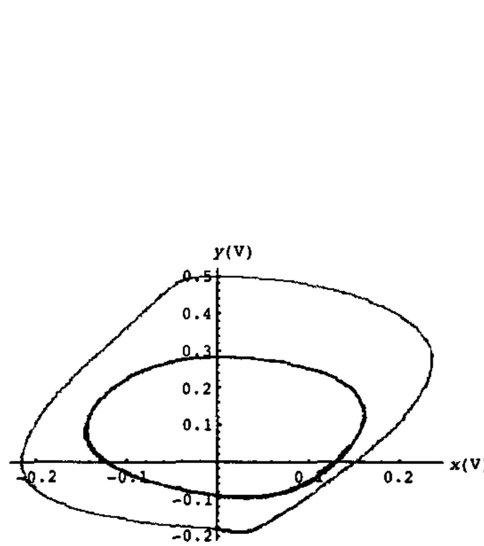

Figure 3. Weak-nonlinear (black curve) and strong-nonlinear (grey curve) oscillatory behavior. The variables x and y are measured from the test oscillator using $x = V_2 \quad V_1$ and $y = V_2 \quad V_{in}$. For the weak-nonlinear curve: $V_{lq} = 0.91$. For the strong-nonlinear curve $V_{lq} = 0.7$. For both curves, $V_b = 0.65$, $V_l = 1.2$.

3. EXPERIMENTAL SYSTEM

Test results are obtained from a CMOS chip fabricated using the TSMC 0.35µm process. The chip contains the coupled oscillator arrays, a test amplifier, and an uncoupled test oscillator. The test amplifier is primarily used to determine the process dependent parameters, so that the physical system can be accurately modeled. A method for time-multiplexing the state variables of each oscillator in the array is implemented by mirroring the output current of the linear amplifiers with shift registers on the periphery of the array and pass devices for each mirrored current. Given the required scanning speeds, a differential current scanning method is used, where currents are switched between lines at identical voltages, thus eliminating the capacitive loading effects of the scanning lines [3][5]. A block diagram of the scanning circuitry is shown in figure 2. The experimental setup consists of a personal computer (PC), a data acquisition card (DAQ), and a microcontroller. The microcontroller is used to interpret commands from the PC, control the scanner clock and data lines for row-column selection, and signal the PC when the scanned output current is ready for measurement. Communication with the microcontroller (Microchip PIC16C84) is handled via I/O ports on the DAC card [National Instruments 6052E]. Commands are received as interrupts on a digital I/O port. The commands are then interpreted as modes. For example, in one mode the microcontroller scans the state of the entire array. Alternatively, there is a mode for scanning rows in the array, and a mode for selecting individual elements. When state variables are scanned from the array the data acquisition card receives a trigger signal from the microcontroller at the start of each frame and each time a new value is available for measurement.

4. WEAK NONLINEAR OSCILLATOR

To better illustrate the behavior of the oscillator it is convenient to express the circuit equations in terms of the van der Pol oscillator, equation (3.0). This is achieved by making a change of variables, so that $x = V_2 \quad V_1$ and $y = V_2 \quad V_{in}$, and by expanding equation (2.0) about x to third order.

$$\ddot{x} = 2 \quad \left(1 \quad x^2\right)\dot{x} \quad {}^2 x \tag{3.0}$$

$$= \frac{1}{2C}\left(A_q B_q \quad A\ B\ \right) \tag{3.1}$$

$$= \frac{A_q{}^3 B_q}{A_q B_q \quad 2A\ B} \tag{3.2}$$

$$= \frac{A\ B}{C} \tag{3.3}$$

In equation (3.0) the parameters , and determine the linearity, the amplitude and frequency of the oscillation respectively. Each of these parameters are fixed by the four parameters A, B, A_q and B_q. Each of these parameters are in tern set by the accessible voltage parameters V_l, V_b, V_{lq} and V_{bq} via equations (1.1) and (1.2).

5. AMPLITUDE AND PHASE MODEL

By considering the weak nonlinear parameter region, where $0 < \quad < 1$, one can take advantage of a separation of time scales and express the oscillator as two independent variables.

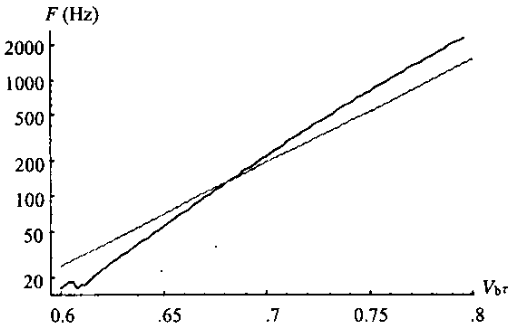

Figure 4. Frequency response of the test oscillator versus bias parameters V_b and V_{bq} (black curve), the parameters are equal through the sweep. Equation (3.3) is also plotted (grey curve). The oscillator has an operational frequency range that spans several orders of magnitude.

The new variables describe the time evolution of a slowly evolving amplitude variable r and a phase variable [6]. The phase-amplitude model is represented by equations (4.0) and (4.1). The solution to equation (4.0) is straight forward. Since this report is concerned with post-transient stable periodic behavior, it is convenient to consider the long time-limit stable amplitude, where $r_* = \frac{2}{\sqrt{}}$

$$\dot{r} = \ 1 \ \frac{}{4} r^2 \ r \qquad (4.0)$$

$$\dot{} = \qquad (4.1)$$

For reference, the phase-amplitude model can be represented by a single complex amplitude equation, equation (5).

$$\dot{a} = (\ + i \ )a \ \frac{}{4}|a|^2 a \qquad (5.0)$$

$$a = re^{i} \qquad (5.1)$$

This description allows a clear understanding of the system dynamics when accessible parameters change. According to equations (3.1)-(3.3) and (1.1)-(1.2) the parameter V_l sets the circuit linear operating region. The parameters V_l, V_b and V_{bq} set the frequency of operation. The parameter V_{lq} is used to set the nonlinearity parameter and the amplitude parameter

Figure 4 illustrates the frequency response of the oscillator as a function of V_b.

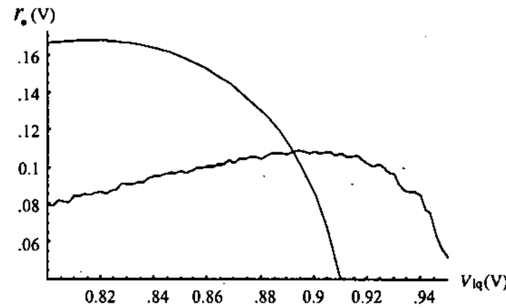

Figure 5. Amplitude response of the oscillator versus the parameter V_{lq} (black curve), which also affects the nonlinearity of the oscillator. The theoretical long-time stability limit for r is also plotted using equation (3.2) (grey curve).

The oscillator natural frequency has a distinctive exponential dependence on the bias parameter and spans several orders of magnitude. Conveniently the frequency of oscillation is independent of the nonlinear feedback parameters. Figure 5 illustrates the amplitude of oscillation as a function of V_{lq}.

This implementation of a phase-amplitude model is a good candidate for studying coupled nonlinear oscillator arrays that function over a wide range of frequencies. In particular, there is recent interest in nonlinear beam-forming arrays. Progress has been made in the construction of nonlinear "shifter-less" beam forming antenna arrays that operate in the gigahertz frequency range. Also, a strong theoretical understanding of similar nonlinear-coupled arrays is forming [1][2]. Such theoretical insight provides a foundation for the precise manipulation of nonlinear arrays. For example, transmit and receive antennas often require a strong main beam and low side lobes in the radiation pattern. This can be achieved by adjusting the stable amplitude of each oscillator in a prescribed way. Nonlinear oscillators that are used to fill these roles will do so successfully if the natural frequency and amplitude can be adjusted independently via accessible parameters. The second-order circuit presented here is one example oscillator.

6. BEAM FORMING ARRAY

Local linear bidirectional coupling is achieved with two additional amplifiers per oscillator, so that the coupling current is proportional to the difference in nearest neighbor V_l variables. The coupled array version of equation (2.0) is given in equation (6.0), along with the coupled van der Pol representation in equation (7.0).

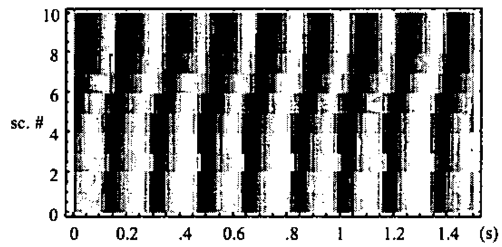

Figure 6. Experimental beam-forming. The beam pattern is obtained by coupling a linear chain of nonlinear oscillators (vertical axis). The variables x_j are plotted as a function of time (bottom axis) and colored using a normalized scale with black and white corresponding to the maximum and minimum amplitude values respectively. Phase shifts between elements in the array occur as a result of frequency detuning each element in the array. Even though each uncoupled oscillator has a unique natural frequency, the oscillators synchronize to a common intermediate frequency due to the coupling and nonlinear qualities of the system. The phase gradient depends on the amount of frequency detuning. The experimental parameters are as follows: $V_t = 1.2$, $V_{lq} = 0.89$, $V_{b,N=1} = 0.55$, $V_{b,N=10} = 0.54$, $V_{bq} = 0.545$.

$$C\dot{V}_{1j} = I_j(V_{in}, V_{1j}) + I_{qj}(V_{1j}, V_{2j}) + I_{cpl}(V_{1j\ 1}, V_{1j}) + I_{cpl}(V_{1j+1}, V_{1j}) \quad (6.0)$$

$$\ddot{x}_j = 2\ {}_j(1\quad {}_jx_j^2)\dot{x}_j\quad {}_j^2x_j + {}_jk(\ {}_{j\ 1}x_{j\ 1} + \dot{x}_{j\ 1} + {}_{j+1}x_{j+1} + \dot{x}_{j+1}\ 2(\ {}_jx_j + \dot{x}_j)) \quad (7.0)$$

$$k = A_{cpl}B_{cpl} \quad (7.1)$$

The array oscillates synchronously with local linear coupling. By frequency detuning each oscillator in the array a stable beam pattern is formed at an intermediate frequency and constant phase difference between oscillators [1][2]. An example time series from the experimental array is shown in figure 6. In the experimental implementation, frequency detuning is achieved by connecting the frequency bias parameters V_b to a resistive voltage divider. By setting the endpoints of the voltage divider a natural frequency gradient is established in the array. For small differences in voltages the gradient is linear. Alternatively the frequency gradient can be established via the parameter V_t. For these results a low operational frequency, on the order of ~10 Hz, is studied due to the low frame rate limitations of the data-acquisition system. From the circuit equations we develop a numerical model of the coupled nonlinear array.

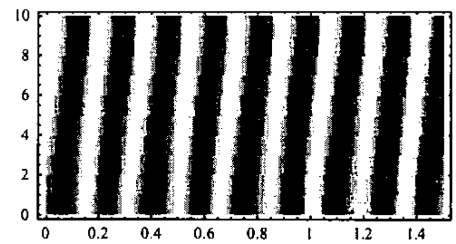

Figure 7. Model beam-forming. The beam pattern is obtained by simulating the coupled circuit equations using a 1st order Euler method. The system dependent parameters are measured directly from the experimental array. The numerical parameters are as follows: $V_t = 1.2$, $V_{lq} = 0.89$, $V_{b,N=1} = 0.551$, $V_{b,N=10} = 0.53$, $V_{bq} = 0.546$.

The numerical model is used as a stopping ground between the analytical predictions and the actual behavior of the array. In its simplest form the numerical model treats the circuit as an ideal system based on equations (2.0) and (2.1). Figure 7 illustrates an example time series from the numerical model. The parameters for the numerical simulation are taken from the experimental parameters.

12. CONCLUSION

These experiments demonstrate the viability of implementing a coupled array of nonlinear oscillators in a practical beam steering application. Issues such as fabrication mismatch between oscillators still present a considerable challenge to creating well-behaved arrays. Future designs will seek to minimize these effects by incorporating more advanced circuit level designs.

12. REFERENCES

[1] T. Heath, K. Wiesenfeld, R. York, "Manipulated synchronization: Beam steering in phased arrays," *Int. J. Bif. Chaos*, vol. 10, pp. 2619-2627, 2000.

[2] T. Heath, "Synchronization and phase dynamics of coupled oscillator," *Ph.D. thesis*, Georgia Tech, 1999.

[3] C. Mead, "Analog VLSI and neural systems," 1989.

[4] S. DeWeerth, G. Patel, "Variable linear-range subthreshold OTA," *Electr. Letters*, 1309 -1311, 1997.

[5] C. Mead, T. Delbruck, "Scanners for visualizing activity of analog VLSI circuitry," *Analog Integrated Circuits and Signal Processing*, 93-106, 1991.

[6] S. Strogatz, "Nonlinear Dynamics and Chaos," *Persius Publishing*, 1994.